Structural assessment of corrosion-damaged RC beams using Finite Element Analysis

Kallias A.N., Rafiq M.I.
Faculty of Engineering and Physical Sciences
University of Surrey
United Kingdom

Abstract

Rebar corrosion is the most frequently observed deterioration mechanism in reinforced concrete (RC), commonly affecting marine, parking and bridge structures. Recently, research efforts have been directed in understanding the effects of corrosion on the performance of RC structures to rationally prioritize the maintenance/repair works. Towards this aim, non-linear finite element analysis (NLFEA) can be used as a tool to simulate the effects of corrosion on the global structural behaviour. In this study, detailed modelling of corroded RC beams is carried out, using 2D-NLFEA. A number of experimentally tested corroded beams are modelled and a good agreement is observed between the numerical load-deflection responses and published data. The numerical models are used to investigate the sensitivity of the predicted response of under-reinforced beams affected by different corrosion damages (i.e. varying corrosion levels, types and locations). The numerical results indicate that the load-deflection curves of the corroded beams are unaffected by impaired bond performance, caused by moderate levels of corrosion. However, notable changes in the predicted cracking patterns and widths are observed. It is also shown that considering the damage of concrete in compression due to corrosion is vital for an accurate structural assessment at both the serviceability (SLS) and ultimate (ULS) limit states. Finally, the results indicate that this modelling approach captures, with sufficient accuracy, the changes in structural response including progressive damage and failure modes.

Keywords: reinforced concrete (RC) modelling, corrosion, NLFEA, bond modelling

1. Introduction

Corrosion of reinforcing steel embedded in concrete causes internal damage to structural elements. The severity of the damage and its influence on structural performance, however, depends on the type, levels and location of corrosion. Corrosion is generally classified as uniform or local (pitting). It may occur at different locations within an element, for instance at the tension, compression and/or shear reinforcements of RC beams. Effects of corrosion include loss of steel area, impaired bond performance, loss of concrete stiffness due to cracking, loss of concrete section due to spalling and reduced mechanical properties for the affected rebars mainly due to pitting formation [1]. When considering the performance of corroded RC beams and slabs, several experimental and analytical studies have been devoted to the area aiming to clarify the influence of each type of corrosion damage on structural response, e.g. see [2-9]. Consistent information regarding the performance of corrosion damaged RC elements could improve the prioritization of inspection/maintenance/repair works and enable the effective use of resources. It is generally accepted that impaired bond performance do not have a significant impact on ultimate load capacity of corroded under-reinforced beams, as soon as the ends of their tension rebars are well-anchored [2, 8]. The effect of bond loss on the serviceability performance, however, is not well established. Experimental evidence suggests that pitting corrosion results in impaired mechanical properties for the affected rebars, including

reduced yield and ultimate strengths as well as ductility, due to localized stress concentrations, e.g. [10]. Experiments on corroded RC beams have shown that pitting corrosion may be responsible for significant reductions in ductility [6, 11]. More recently, the effect of concrete damage, due to corrosion, in the compressive zone of RC beams was investigated experimentally [6] and analytically [12]. Also, proposals for the inclusion of this type of damage in the assessment of corroded beams were made, e.g. [8]. Despite these efforts, the effect of concrete damage in compression on the structural performance of under-reinforced beams is not clear in literature. In the experimental study of [6] the effect of concrete damage in compression is investigated, but limited to over and balanced reinforced beams. No results were presented for under-reinforced beams. In the numerical study presented in [8], although concrete damage in the compressive zone of beam is considered in the analysis, the examined beams were affected by several types of corrosion. As a result it was not possible to distinguish, to which extent the beam performance was affected by damage of concrete in compression. In the present study, a methodology is presented suitable for the assessment of corroded RC beams using NLFEA in the FE program DIANA. The main effects of corrosion are recognized and considered in the analysis. A number of uncorroded and corroded beams from two independent experimental studies are modelled and analyzed and a good correlation between the numerical and experimental results is observed. Thereafter, the numerical models are used to assess the impact of different effects of corrosion and their associated assumptions on the predicted response through a number of analysis cases.

2. Description of examined RC beams

RC beams from two published experimental studies are selected for this study [3, 6]. In both cases, one of the beams served as control specimen, while beams of similar geometrical characteristics were subjected to different levels of corrosion using accelerated corrosion techniques. The geometrical characteristics of the examined beams are schematically depicted in Fig.1, while the corresponding dimensions, reinforcement detailing, material properties and values of corrosion current used are tabulated in Table 1.

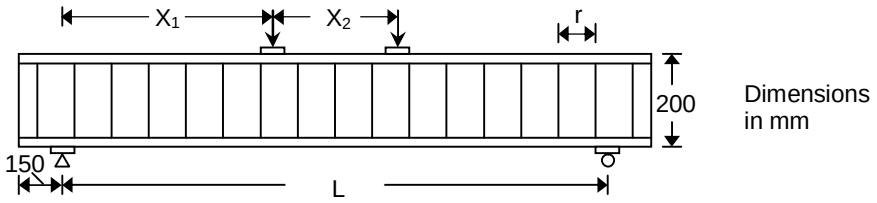

Fig.1: Geometrical characteristics of the examined beams, see also Table 1

The S116 beam had all its rebars (along the entire length) affected by corrosion [3, 11]. Beam T282 [6] was partly corroded, over a centrally 600mm length in the region of its tensile rebars.

Table 1: Geometrical details and material properties of sample corroded beams examined

Beams		Steel ratio (%)	L (mm)	Beam width (mm)	Loads spacing X_1/X_2 (mm)	Reinforcing bars			Concrete compr. strength (MPa)	Corrosion current ($\mu A/cm^2$)
						Tension No/diameter/ yield strength (no/mm/MPa)	*Compression* No/diameter/ yield strength (no/mm/MPa)	*Links* diameter/spacing/ yield strength (mm/mm/MPa)		
Ref. [3]	S111	0.5	2000	150	800/400	2/10/575	2/8/615	6/170/615	50	–
	S116	0.5	2000	150	800/400	2/10/575	2/8/615	6/170/615	34	100
Ref. [6]	T280	0.87	1800	150	750/300	2/12/489	2/8/526	8/170/615	35.8	–
	T282	0.87	1800	150	750/300	2/12/489	2/8/526	8/170/615	44.5	350

3. Modelling the effects of corrosion

Corrosion may occur at different locations in an RC element. It leads to progressive internal damage of the affected RC element. The extent of overall impairment of a concrete element, however, depends on the type, location and levels of corrosion, which should be considered in the assessment. The following effects of corrosion are considered in this study:

- Loss of steel area due to uniform corrosion damage;
- Reduced yield-strength due to the presence of pitting corrosion on the affected rebars;

- Impaired bond performance due to corrosion of the main rebars and confining stirrups;
- Residual mechanical properties/area loss of concrete in compression due to uniform corrosion of the compressive rebars;

3.1 Loss of steel area and residual yield strength

Corrosion may physically affect steel reinforcement in the following two ways: (a) causing a relatively uniform loss of steel area and (b) by the formation and propagation of localized defects, namely pitting corrosion. The former type of corrosion doesn't affect much the stress-strain behaviour of the affected rebars and it can be modelled by reducing the area of the truss elements representing steel. In contrary, pitting corrosion may cause alteration of the apparent behaviour of a rebar. More specifically, the formation of localised defects causes stress concentrations, which in turn lead to localised rebar yielding and rapture [11]. As a result the average stress level in the rebar at yielding appears to be lower than the yield stress of intact rebars. This behaviour tends to be more evident as levels of corrosion increase. In the present study, a reduced yield strength is considered using Eq.1, which assumes a linear reduction of yielding stress for increasing corrosion levels [13].

$$f_y^D = \left[1.0 - \alpha_y \left(A_{pit}/A_{stnom}\right)100\right] f_y \qquad (1)$$

Where, f_y^D=reduced yield strength, f_y=initial yield strength, A_{stnom}=cross-sectional area of uncorroded rebar, D_o=initial diameter of the rebar, α_y=empirical coefficient=0.005 and A_{pit}=pit area, which is a function of depth and width of the pit and D_o, for details see [13]. In the case that an accurate assessment of ductility is required, similar strength and strain reduction factors should be employed, to evaluate the residual (ductility) properties of the tensile corroded rebars, for instance see [10].

3.2 Modelling of residual bond properties

3.2.1 Bond strength of corroded rebars

Experimental evidence suggests that bond between the tensile longitudinal reinforcement and concrete may be affected by corrosion in the following ways [1, 14]:

- At low corrosion levels an increase in bond strength is observed. Bond deterioration occurs following the formation of longitudinal corrosion cracks along the length of the affected rebar;
- The levels of confinement directly affects the residual bond properties of corroded rebars;
- Stirrup corrosion results in reduced stirrup area and mechanical properties as well as concrete cover cracking and spalling. Thus, stirrup corrosion may cause reduction of bond performance of an anchored rebar even if the latter is unaffected by corrosion, due to reduced confinement;

Modelling the interaction of corroded rebars in tension with concrete, should consider the changes of concrete and stirrup contributions towards bond performance. In the present study the bond strength for corroded rebars, is calculated using Eq.2 [5]:

$$u_{\max} = R\left[0.55 + 0.24\left(c/d_b\right)\right]\sqrt{f_c} + 0.191\left[A_{st} f_{yt}/s d_b\right] \qquad (2)$$

Where, c=thickness of concrete cover, d_b=rebar of anchored rebar, f_c=concrete compressive strength, A_{st}=area of shear reinforcement, f_{yt}=yield strength of stirrups, s=stirrup spacing, $R=A_1+A_2X$=corrosion factor to account for changed contribution of concrete towards bond performance, X=levels of corrosion of the anchored rebar, A_1 & A_2=factors depending on the current used during the corrosion period, for details see [5]. In Eq.2, reductions in confinement to the main rebars due to stirrup corrosion are taken into account by reducing the stirrup area and yield-strength. An advantage of the selected bond strength model, over previously proposed models [15], is its ability to capture an initial increase of bond strength, observed experimentally for low levels of corrosion, e.g. [16].

3.2.2 Local bond stress-slip law

The bond behaviour of uncorroded and corroded rebars in tension embedded in concrete is described by means of a local bond stress-slip relationship. In the present study the local bond stress-slip proposed by Harajli et al. [17], is modified to account for the effects of corrosion, see Fig.2 (d), for details of the proposed modification see [18]. The local bond stress-slip relationship is used as originally proposed in [17] for the modelling of bond in the control beams. The ascending part of the curve is described by a relation similar to the one proposed by MC90 [21] with a slightly different coefficient, while the slip at which bond strength is mobilized is given by Eq.(3), see Fig.2 (d):

Slip at bond strength: $$s_{\max} = s_1 e^{(1/0.3)Ln(u_{\max}/u_1)} + s_0 Ln\left(u_1/u_{\max}\right) \quad (3)$$

Where: u_1=2.57$(f_c)^{0.5}$, f_c=compressive strength of concrete, s_1=0.15c_0, s_2=0.35c_0, c_0=clear rib spacing=8mm (assumed) and s_0=0.4. The selected bond-slip law predicts an initial stiff bond response. As bond stress approaches bond strength, a reduction in bond stiffness is observed, i.e. 0.7u_{max} at slip s_a. Subsequently, bond stress reduces linearly to zero at slip s_2. The selected local bond stress-slip relationship is in good agreement with experimental data [18-19].

3.3 Residual mechanical properties of concrete in compression

The formation and accumulation of expansive corrosion products at the steel-concrete interface leads to microcracking, cracking and eventually spalling of the surrounding concrete. Damage concrete subjected to compressive stresses is likely to exhibit impaired performance compared to undamaged concrete, i.e. reduced strength and ductility. To account for such damage in the analysis, a methodology proposed in [8] is adopted in which a reduced strength is calculated using Eq. (4):

$$f_c^D = \frac{f_c}{1 + k\left(\varepsilon_1/\varepsilon_{co}\right)} \quad (4)$$

Where, f_c^D=residual concrete strength, f_c=compressive strength of undamaged concrete, k=0.1, ε_{co}=concrete deformation at peak load, ε_1=smeared transverse strain due to corrosion cracking. ε_1 is calculated as a function of the number of corroded bars in a section, the volumetric expansion ratio of the corrosion products and the replaced steel and the average attack penetration, for details see [8].

4. Two-dimensional finite element modelling of RC beams

4.1 Concrete modelling

4.1.1 Behaviour in tension

In the present study, concrete in tension is modelled using a standard rotating smeared crack model with tension softening. The crack band model is used as localization limiter. A relatively fine mesh is used (i.e. 10x10mm), in which discrete cracks can obtained by visualization of the softened (cracked) concrete elements. The non-linear softening curve of Hordijk et al., see Fig.2 (b), is adopted as described and implemented in the FE code DIANA [20]. All the required input parameters, such as Mode I fracture energy, G_F and tensile strength of concrete, are obtained from MC90 based of the concrete compressive strength and maximum aggregate size [21].

4.1.2 Behaviour in compression

The behaviour of concrete in compression is modelled using a parabolic curve as shown in Fig.2 (a). A linear elastic behaviour is assumed for stress levels up to 30% of its compressive strength f_c. Thereafter, its behaviour becomes non-linear until f_c is reached. In this formulation the post peak-response of concrete in compression (i.e. softening in compression) is modelled using compressive fracture energy, G_c. This parameter is obtained according to the recommendations provided in [22]. In beams with corrosion damage affecting their rebars in compression, a reduced compressive strength and ductility is adopted for the concrete of the top cover as previously discussed. In the present study, this type of corrosion damage is assumed to affect only the elements of the top cover; other studies, however, have suggested that the depth of the damaged zone should extent below the depth of the longitudinal compressive rebars [12].

4.2 Steel reinforcement

All embedded rebars are modelled using one-dimensional truss elements and their behaviour is assumed to be elastic-perfectly plastic, see Fig.2 (c) and (e). A reduced steel area and yield strength are used for the corroded rebars using a methodology discussed earlier in this paper.

4.3 Bond

Bond between the tensile rebars and concrete is modelled in both the control and corroded beams using two-dimensional (2D) interface elements. Since bond behaviour is considered only in the direction along the longitudinal axis of the rebars a zero thickness is assigned to the interface elements, which reduces them to 1D, for details see Fig.2 (f) and (g).

4.4 Loading and analysis procedure

The beams are loaded using two symmetric monotonically increasing concentrated loads in a four-point bending configuration as shown in Fig.1. A regular Newton-Raphson iterative algorithm is used in which loading is applied by means of a displacement control.

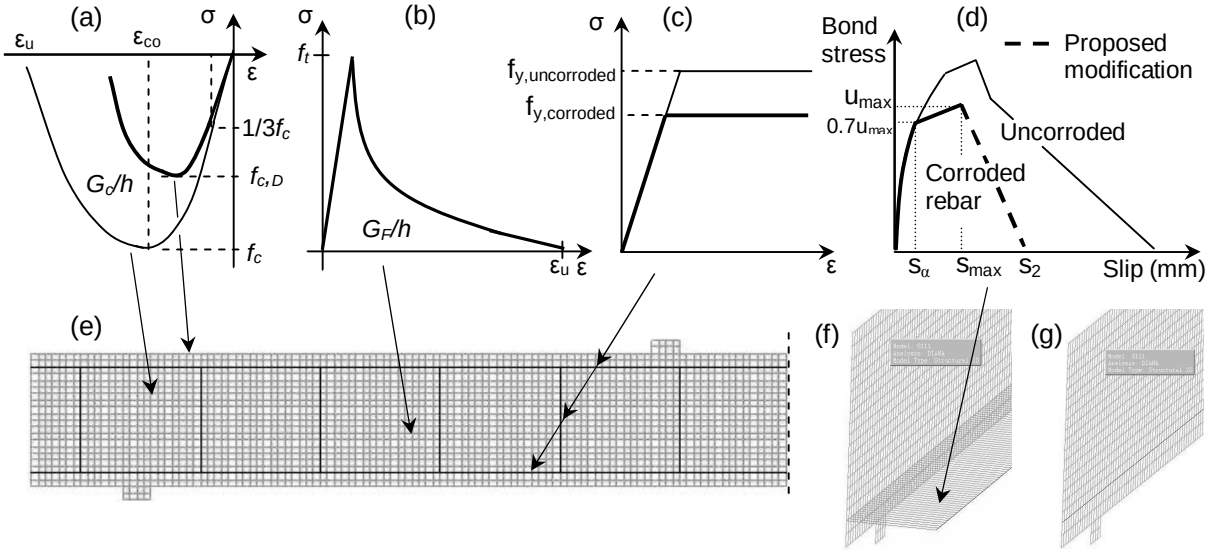

Fig.2: Models for concrete in (a) compression, (b) tension, (c) steel rebars, (d) bond and typical mesh discretization: (e) half beam, (f) interface elements (g) assignment of zero thickness to interface elements

5. Analysis cases and parameter variation

The analysis cases considered in the present study and details of the parameter variation are summarized in Table 2 below:

Table 2: Summary of sample analysis cases and parameter variation

Beam	Description
S111	Uncorroded, bond strength according to [5], bond-slip according to [17]
S116a	Steel area loss, reduced yield strength, bond, and strength/ductility of top cover, loss of side covers
S116b	Steel area loss, reduced yield strength and bond, intact top and side covers
S116c	Steel area loss, reduced yield strength and strength/ductility of top cover, no bond deterioration
T280	Uncorroded, bond strength according to [5], bond-slip [17]
T282	Steel area loss, reduced yield strength and bond

6. Results and discussion

Fig.3 shows a comparison between the numerical and experimental results for the S-type uncorroded and corroded beams, in which a good correlation between experimental and numerical results is observed. Examination of the results revealed that corrosion caused significant deterioration of structural performance, where the reduction of yield and ultimate loads is more than 40%, see Fig.3. The response of control beam S111 is characterised by the formation of flexural cracks at load-levels corresponding to 35% of its ultimate load. Failure in this beam occurred by means of steel yielding, which was followed by concrete crushing under sustained loads. In contrary, the corroded beam S116a exhibits an altered response compared to the control beam, see Fig. 3. As the levels of corrosion increased, shear cracks formed in the more corroded beams S116a. No shear failure, however, occurred in any of the analyses. In beam S116a, although bond failure occurred locally (over small portions along the rebar), its effect on performance was little, affecting slightly the stiffness and primarily the cracking patterns obtained.

It was noted that modelling the damage of the concrete in compression was crucial for the accurate prediction of strength and stiffness. More specifically, as the load increased, the concrete cover in compression started to crush gradually. The FE model predicted that the concrete damage (i.e. concrete crushing) in the top cover localised in a few elements, which is a satisfactory behaviour from a physical point of view.

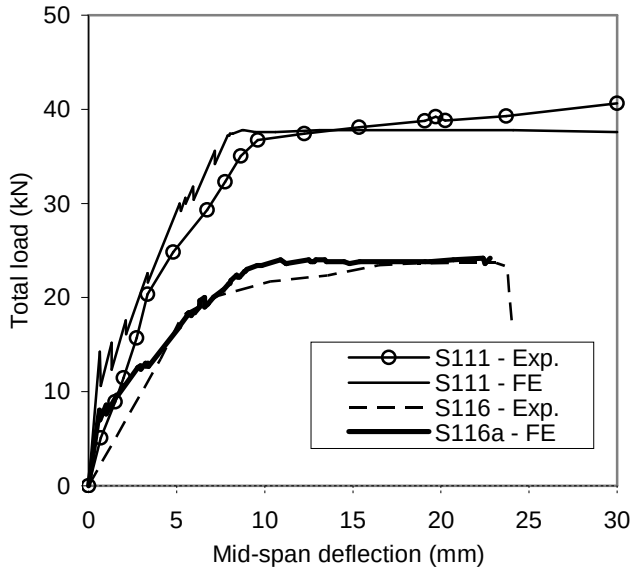

Fig.3: Numerical and experimental load-deflection curves for beamS S111 (control) and S116a

As previously discussed, all the rebars of S116 beam are affected by corrosion. As a result, it is difficult to separate the impact of each type of corrosion damage on structural response. To investigate the impact of bond loss in the predicted response, beams T280 and T282 are modelled and analysed. Beam T280 serves as the control specimen (uncorroded), while in beam T282 corrosion was induced only over a central portion (one third the length of the clear span) of the tensile rebars, with all other rebars being uncorroded. The numerical results for beams T280 and T282 are shown in Fig.4 (a). As it can be seen in Fig.4 (a) corrosion damage in the tensile rebars of beam T282, caused an approximately 10% reduction of both yield and ultimate loads. Additionally, notable changes in cracking patterns and widths are observed; see in Fig.4 (b). As it can be seen, a reduced number of flexural cracks formed in the corroded beam T282 at loads levels corresponding to the serviceability limit, with their widths being much larger than the cracks predicted for the uncorroded beam T280. This observation is in agreement with published experimental data, for instance see [11]. The numerical results indicate that the load-deflection response of corroded beam T282 is unaffected by moderate damage in bond performance. Consequently, strength reductions observed in beam T282 are attributed to loss of tensile steel area and not to the loss of bond. This observation is supported by experimental evidence [6], where a 10% strength reduction without stiffness deterioration is observed in the load-deflection response of the corroded beam T282, see Fig.4 (a).

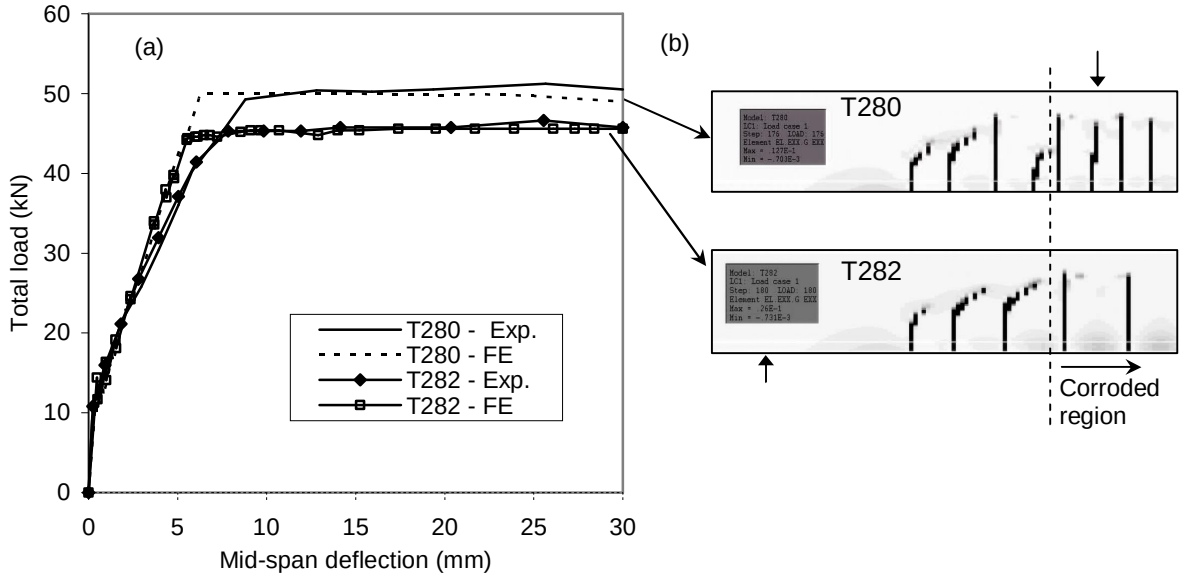

Fig.4: Experimental and numerical results for beams T280, T282a and T282b: (a) Load-deflection curves and (b) cracking patterns at service load (showing half beam)

An additional analysis case (i.e. model S116c) of the severely corroded beam S116 considers the sensitivity of bond deterioration on load-deflection response. No deterioration of bond is considered in this numerical model, which is otherwise similar to model S116a. A comparison of the numerical results for beams S116a and S116c are shown in Fig.5 (showing only the initial part of the load-deflection curves). It can be seen that the overall performance is not significantly affected by bond deterioration. Changes in the predicted cracking patterns are observed between numerical models

S116a and S116c, which follow a similar trend to the cracking patterns obtained for beams T280 and T282, i.e. bond deterioration resulted in increased crack spacing and widths. Further examination of the results shows that assuming no bond deterioration in beam S116c, concrete crushing initiates, slightly earlier than for beam S116a, see Fig.5. This indicates that an interaction exists between the different types of corrosion damage occurred at the tension and compressive zones of the beam.

Finally, the numerical results of beam S116b indicate that considering no concrete damage in the top cover, due to corrosion, causes overestimation of strength and stiffness, see Table 3, alongside higher bond demand (than beam S116a) for the corroded tensile rebars.

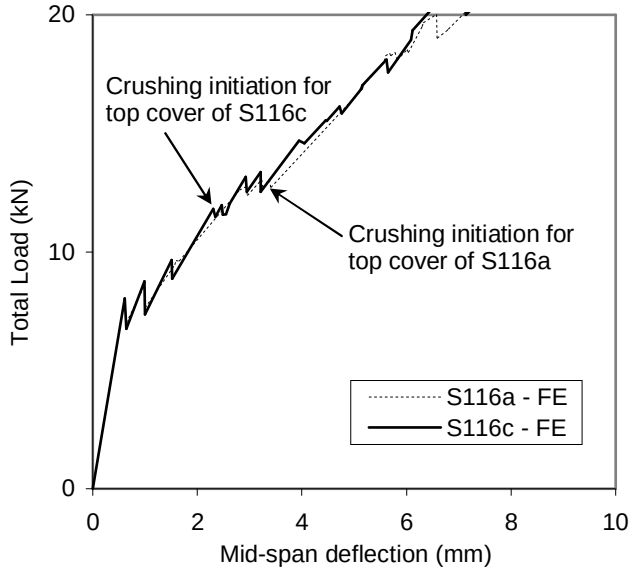

Fig.5: Numerical load-deflection curves for beams S116a and S116c (showing only the initial part of the curves)

Table 3: Summary of FE results from analysis cases for beams S111, S116a and S116b

Beam	Load at yielding (kN)		Failure load (kN)		Deflection at service load (mm)	
	Num.	Exp.	Num.	Exp.	Num.	Exp.
S111	38.6	38.4	37.6	40.6	2.9	3.3
S116a	23.1	21.5	24.2	23.6	7.1	7.1
S116b	27.2	21.5	28.2	23.6	4.9	7.1

7. Conclusions

In this study detailed modelling of corrosion damaged RC beams was carried out using 2D-NLFEA. A number of uncorroded and corroded beams have been modelled using the FE code DIANA and a good correlation is observed between the experimental and numerical results. A sensitivity study is carried out, using the numerical models, to examine the impact of different modelling assumptions on the computed response. The following conclusions may be drawn from this investigation:

- → The results indicate that corrosion damage can cause significant impairment of structural performance; furthermore, the importance of considering the main effects of corrosion in the structural assessment of damaged RC structures was confirmed;
- → Corrosion related bond degradation has a little effect on the load-deflection response of corroded beams, where their tension rebars are damaged by moderate levels of corrosion. This observation is in agreement with previous studies. Notable changes, however, in the cracking patterns and widths, due to impaired bond, are observed, due to loss of tension stiffening;
- → The result indicate that considering the damage of concrete in compression due to corrosion is vital for an accurate structural assessment at both the serviceability (SLS) and ultimate (ULS) limit states;
- → The response (i.e. strength, stiffness etc) of corroded beams is likely to be notably affected by damage of the concrete in compression due to corrosion. As a result the loss of steel area and concrete section are found to be responsible for the observed stiffness and strength reductions;
- → Finally, the results indicate a possible interaction between the corrosion damage in the compression and tension regions of RC beams. It was noted that concrete damage due to corrosion in the compression region of a beam may cause a reduced bond demand for the tensile rebars.

Acknowledgments
The support grant (DTG) provided by EPSRC and the provision of required facilities by the University of Surrey, are both gratefully acknowledged. The authors would like to acknowledge the support and valuable discussions with Prof. M. Chryssanthopoulos from the University of Surrey, UK.

References
[1] FIB, "*Bond of reinforcement in concrete, State-of-art report*", fib bulletin 10, Federation Internationale du Beton, prepared by Task Group Bond Models, Lausanne, 2000
[2] Cairns J., Zhao Z., "Behaviour of concrete beams with exposed reinforcement", Proceedings of the Institution of Civil Engineers, Structures and Buildings 99(2), 1993, pp.141-154
[3] Rodriguez J., Ortega L.M., Casal J., "Load carrying capacity of concrete structures with corroded reinforcement", Construction and Building Materials 11(4), 1997, pp.239-248
[4] Mangat P.S., Elgarf M.S., "Flexural strength of concrete beams with corroding reinforcement", ACI Structural Journal 96(1), 1999, pp.149-159
[5] Maaddawy T.E., Soudki K., Topper T., "Analytical model to predict nonlinear flexural behaviour of corroded reinforced concrete beams", ACI Structural Journal 102(4), 2005, pp.550-559
[6] Du Y., Clark L.A., Chan A.H.C., "Impact of reinforcement corrosion on ductile behaviour of reinforced concrete beams", *ACI Structural Journal* 104(3), 2007, pp.285-293
[7] Chung L., Najm H., Balaguru P., "Flexural behaviour of concrete slabs with corroded bars", Cement & Concrete Composites 30, 2008, pp.184-193
[8] Coronelli D., Gambarova P., "Structural assessment of corroded reinforced concrete beams: modelling guidelines", Journal of Structural Engineering 130(8), 2004, pp.1214-1224
[9] Toongoenthong K., Maekawa K., "Multi-mechanical approach to structural assessment of corroded RC members in shear", Journal of Advanced Concrete Technology 3(1), 2005, pp.107-122
[10] Cairns J., Plizzari G.A., Du Y., Law D.W., Franzoni C., "Mechanical properties of corrosion-damaged reinforcement", ACI Materials Journal 102(4), 2005, pp.256-264
[11] Rodriguez J., Ortega L.M., Casal J., Diez J.M., "Assessing structural conditions of concrete structures with corroded reinforcement", in *Concrete Repair, Rehabilitation and Protection*, Dhir and Jones (Editors), E&FN Spon, 1996, ISBN 0-419-21490-9
[12] Capozucca R., Cerri M.N., "Influence of reinforcement corrosion – in the compressive zone – on the behaviour of RC beams", Engineering Structures 25, 2003, pp.1575-1583
[13] Stewart M.G., "Mechanical behaviour of pitting corrosion of flexural and shear reinforcement and its effect on structural reliability of corroding RC beams, Structural Safety 31(1), 2009, pp.19-30
[14] Lundgren K., "Effect of corrosion on the bond between steel and concrete: an Overview", Magazine of Concrete Research 59(6), 2007, pp.447-461
[15] Rodriguez J., Ortega L.M., Casal J., "Corrosion of reinforcing bar and service life of reinforced concrete structures: Corrosion and bond deterioration", Proc. Int. Conf. on Concrete Across borders, Vol.2, 1994, pp.315-326
[16] Almusallam A.A., Al-Gahtani A.S., Aziz A.R., Rasheeduzzafar, (1996), "Effect of reinforcement corrosion on bond strength", Construction and Building Materials 10, pp.123-129
[17] Harajli M.H., Hamad B.S., Rteil A.A., "Effect of confinement on bond strength between steel and concrete", ACI Structural Journal 101(5), 2004, pp.595-603
[18] Kallias A.N., Rafiq M.I., (2009), "Assessment of corroded RC beams: The effect of corrosion damage in the compression zone", To be submitted for publication
[19] Fang C., Lundgren K., Chen L., Zhu C., "Corrosion influence on bond in reinforced concrete", Cement and Concrete Research 34, 2004, pp.2159-2167
[20] TNO, "DIANA 9.1 User's Manual", TNO Building and Construction Research, 2005, Delft
[21] CEB, "*CEB-FIP Model Code 1990*", Bulletin d'Information 213/214, 1993, Lausanne, Switzerland
[22] Nakamura H., Higai T., "Compressive fracture energy and fracture zone length of concrete", in *Modelling of inelastic behaviour of RC structures under seismic loads*, Shing P., Tanabe T. (Eds), American Society of Civil Engineers, 2001, pp.471-487